Vibrations of the S1 state of fluorobenzene-h 5 and fluorobenzene-d 5 via resonance-enhanced multiphoton ionization (REMPI) spectroscopy

Joe P. Harris, Anna Andrejeva, William D. Tuttle, Igor Pugliesi, Christian Schriever, and Timothy G. Wright

Citation: The Journal of Chemical Physics **141**, 244315 (2014); doi: 10.1063/1.4904706
View online: http://dx.doi.org/10.1063/1.4904706
View Table of Contents: http://scitation.aip.org/content/aip/journal/jcp/141/24?ver=pdfcov
Published by the AIP Publishing

Vibrations of the S_1 state of fluorobenzene-h_5 and fluorobenzene-d_5 via resonance-enhanced multiphoton ionization (REMPI) spectroscopy

Joe P. Harris,[1] Anna Andrejeva,[1] William D. Tuttle,[1] Igor Pugliesi,[2] Christian Schriever,[2] and Timothy G. Wright[1,a)]

[1]*School of Chemistry, University of Nottingham, University Park, Nottingham NG7 2RD, United Kingdom*
[2]*Lehrstuhl für BioMolekulare Optik, Ludwig-Maximilians-Universität München, Oettingenstr. 67, 80538 München, Germany*

(Received 24 October 2014; accepted 8 December 2014; published online 31 December 2014)

We report resonance-enhanced multiphoton ionization spectra of the isotopologues fluorobenzene-h_5 and fluorobenzene-d_5. By making use of quantum chemical calculations, the changes in the wavenumber of the vibrational modes upon deuteration are examined. Additionally, the mixing of vibrational modes both between isotopologues and also between the two electronic states is discussed. The isotopic shifts lead to dramatic changes in the appearance of the spectrum as vibrations shift in and out of Fermi resonance. Assignments of the majority of the fluorobenzene-d_5 observed bands are provided, aided by previous results on fluorobenzene-h_5. © *2014 AIP Publishing LLC.* [http://dx.doi.org/10.1063/1.4904706]

I. INTRODUCTION

Fluorobenzene-h_5 is, of course, one of the simplest substituted benzenes. The key pieces of early work that focus on the vibrational spectroscopy of the ground, S_0, state are those of Whiffen[1] (and references therein) and, somewhat later, Lipp and Seliskar.[2] These led to the assignment of many of the vibrational modes by virtue of the measured frequency, as well as a deduction of their symmetry from the appearance of the rotational contour. More recent work has essentially confirmed these assignments, with only minor refinements, often with the aid of quantum chemical calculations. More recently, Scotoni *et al.*[3] have recorded IR spectra in the region of some of the CH stretches, allowing them to investigate interactions between these modes. A summary of the work in this area has been provided by us recently.[4] However, as noted in Ref. 4, the nomenclature has often been in terms of Wilson notation,[5] based upon the vibrations of benzene, which can change considerably upon substitution. The latter issue has been described in detail for fluorobenzene by Pugliesi *et al.*,[6] where it was noted that the Wilson labels were inappropriate, owing to the widespread mixing between the ring-localized vibrations. There are also limitations of the Varsányi notation[7] owing to a somewhat arbitrary division of the substituents into heavy or light groups, which leads to similar vibrations having different labels, even between quite similar species. Better, for fluorobenzene-h_5 is the Herzberg notation[8] (also known as Mulliken notation from his recommendations[9]), based upon a wavenumber-ordered numbering of the vibrations in symmetry blocks. In Ref. 4, we noted that the Herzberg (Mulliken) labels had limited use when comparing between substituted benzenes, particularly when the substitution led to other vibrations and/or a different point group, which altered the numbering. To address this, we put forward[4] a consistent method of labelling the ring-localized vibrational modes of the monosubstituted benzenes, which leads to the same vibrational mode having the same label, M_i, no matter what the substituent is. We applied this in the case of toluene,[10] and showed that the vibrational activity observed in the $S_1 \leftarrow S_0$ transition was very similar for fluorobenzene and chlorobenzene, as well as toluene-d_3, as expected. We note that the M_i labels are precisely the Herzberg (Mulliken) labels for the S_0 state of fluorobenzene-h_5, by construction; the motions of the atoms in each mode may be seen in the diagrams presented in Ref. 4.

The vibrational spectroscopy of the S_0 state of the fluorobenzene-d_5 isotopologue has been reported by Steele *et al.*[11] employing both IR and Raman spectroscopies. Fundamental vibrational wavenumbers were reported for 24 of the 30 vibrations. These were largely confirmed by Lipp and Seliskar in 1978 in a higher resolution study.[2] Only approximate mode descriptions were offered by Steele *et al.*[11] but these were assigned labels based on the Wilson nomenclature by Varsányi.[7] Also, Lipp and Seliskar[2] provided Wilson labels, some of which were different to those proposed by Varsányi—we shall come back to this later.

The electronic spectroscopy of fluorobenzene-h_5 has been studied for very many years, stretching back to at least 1946.[12] A two-photon spectrum by Vasudev and Brand was reported in 1979,[13] where different activity from the one-photon spectrum was reported. A comprehensive study of the $S_1 \leftarrow S_0$ transition of fluorobenzene was reported by Lipp and Seliskar[14] in the early 1980s using UV absorption spectroscopy, where bands were identified by expected wavenumber and rotational contour type; a partner paper described the hot band features.[15] Additionally, in 2005, the shift of the origin of the electronic spectrum of fluorobenzene entrained in helium nanodroplets was reported.[16] In 2007, a very thorough laser induced

a)Author to whom correspondence should be addressed. Electronic mail: Tim.Wright@nottingham.ac.uk

fluorescence study was carried out by Butler *et al.*,[17] where activity in dispersed fluorescence (DF) spectra was used to confirm assignments of bands. Unusual vibrational activity in the spectrum was discussed in terms of Duschinsky rotation and anharmonic vibrational coupling, such as Fermi resonances. The following year, a detailed analysis of the lower wavenumber region of the same transition was carried out employing resonance-enhanced multiphoton ionization (REMPI) spectroscopy, coupled with spectral simulation and zero-kinetic-energy (ZEKE) spectroscopy;[6] activity in the latter spectra could be used to confirm assignments of the S_1 vibrational structure, in a similar way to dispersed fluorescence. Very recently, Gascooke *et al.*[18] used this transition in fluorobenzene to demonstrate the two-dimensional laser-induced fluorescence (2D-LIF) technique, showing it to be a powerful tool in unravelling overlapping structure and vibrational couplings; it was also possible to identify structure arising from naturally occurring isotopologues.

Here, we concentrate on the $S_1 \leftarrow S_0$ transition for the isotopologues fluorobenzene-h_5 and fluorobenzene-d_5. For brevity, we refer to these by the following abbreviated forms in the below: FBz-h_5 and FBz-d_5. We employ one-colour REMPI spectroscopy, and assign the spectra employing previous results, plus expected shifts based on quantum chemical calculations. Essentially, we confirm the assignments of the FBz-h_5 vibrational features; the REMPI spectrum for FBz-d_5 is reported here for the first time. In order to compare the vibrational assignments of both isotopologues in the S_0 state, we consider the mixing of vibrational modes which occurs as the masses of all the hydrogen atoms are artificially changed from 1 amu through 2 amu (i.e., as the vibrations of FBz-h_5 transform into the FBz-d_5 ones). We subsequently highlight the mixing of the vibrational modes that occurs between the S_0 and S_1 states for each isotopologue.

II. EXPERIMENT

The third (355 nm) harmonic of a neodymium-doped yttrium aluminium garnet laser (Nd:YAG, Surelite III, 10 Hz) was used to pump a tuneable dye laser (Sirah Cobra Stretch), operating on Coumarin 503. The fundamental output of the dye laser was frequency doubled using a beta-barium borate (BBO) crystal to allow tuneable UV radiation to be produced across the wavenumber regions of interest.

The vapour above fluorobenzene-h_5 (Aldrich, 99.8% purity) or fluorobenzene-d_5 (Aldrich, 99 at. % D) was seeded in 2–5 bar of argon carrier gas and the gaseous mixture was passed through a general valve pulsed nozzle (750 μm, 10 Hz, opening time of 150–200 μs) to create a free jet expansion. The focused, frequency-doubled output of the dye laser passed through a vacuum chamber where it intersected the free jet expansion perpendicularly, between two biased electrical grids located in the extraction region of a time-of-flight spectrometer. Here, (1 + 1) ionization occurred and the resulting ions were extracted and subsequently detected by a dual microchannel plate detector. The signal was passed to an oscilloscope (LeCroy LT342 Waverunner) for monitoring, and a boxcar (SRS SR250) for integrating and averaging; this signal was then relayed to a computer for storage and analysis. The timing of the laser pulse relative to the opening time of the pulsed nozzle was controlled using a digital delay generator (SRS DG535). The delays were varied to produce optimum conditions, so that the coldest part of the free jet expansion was probed.

The calibration was performed by comparison of the S_1 origin band of FBz-h_5 observed in the present work to previous UV absorption spectra.[14] We estimate that our overall uncertainty in band positions is ±1 cm^{-1} and 0.2 cm^{-1} in relative band positions.

III. COMPUTATIONAL METHODOLOGY

In order to aid in the assignment of the spectra, the vibrational frequencies of the two isotopologues of fluorobenzene were calculated using the GAUSSIAN 09 software package.[19] For the S_0 ($\tilde{X}^1A_1$) state, B3LYP/aug-cc-pVTZ calculations were used, while for the S_1 ($\tilde{A}^1B_2$) state, we employed TD-B3LYP/aug-cc-pVTZ calculations.

All of the calculated harmonic vibrational wavenumbers were scaled by the usual factor of 0.97. We note that in our recent work on toluene,[10,20] we found that these scaled harmonic values were at least as reliable as the explicitly calculated anharmonic values (with the latter being very expensive to calculate). The S_0 vibrational modes of FBz-h_5 have been labelled as described in Ref. 4 according to the usual Mulliken/Herzberg recipe, providing a clear assignment of the vibrations—the forms of the vibrations can also be seen in that work. Here, we compare the FBz-d_5 molecular vibrational motions with those of FBz-h_5 using a generalized Duschinsky matrix approach, and also compare S_0 and S_1 vibrational modes for the corresponding isotopologues. These Duschinsky-mixing matrices were obtained with the FC-LabII program;[21] however, a modification of the code was employed for the isotopologues to provide for more reliable normalization of the resulting matrices. (In Ref. 4, when normalization issues arose, we addressed this by manual normalization of rows and/or columns; tests using the new version of the program confirm that the latter procedure gives almost the same results, but the use of the new version of the program is much more efficient and reliable.)

IV. RESULTS AND ASSIGNMENTS

A. Overview of $S_1 \leftarrow S_0$ spectra

An overview of the (1 + 1) REMPI spectrum of both FBz-h_5 and FBz-d_5 (inverted trace) is shown in Figure 1. The origin band of FBz-h_5 is located at 37 816.2 ± 1 cm^{-1} and at 37 989.8 ± 1 cm^{-1} for FBz-d_5. We have calibrated our spectra to the FBz-h_5 spectrum reported by Lipp and Seliskar,[14] which also then puts our FBz-d_5 origin in agreement with theirs to within 1 cm^{-1}. For FBz-h_5, the origin value also agrees with that given by Pugliesi *et al.*,[6] and is in reasonable agreement with that from Butler *et al.*[17] Since our bands are not fully rotationally resolved, we have taken the position of an observed dip in the band profile of the coldest spectra to be indicative

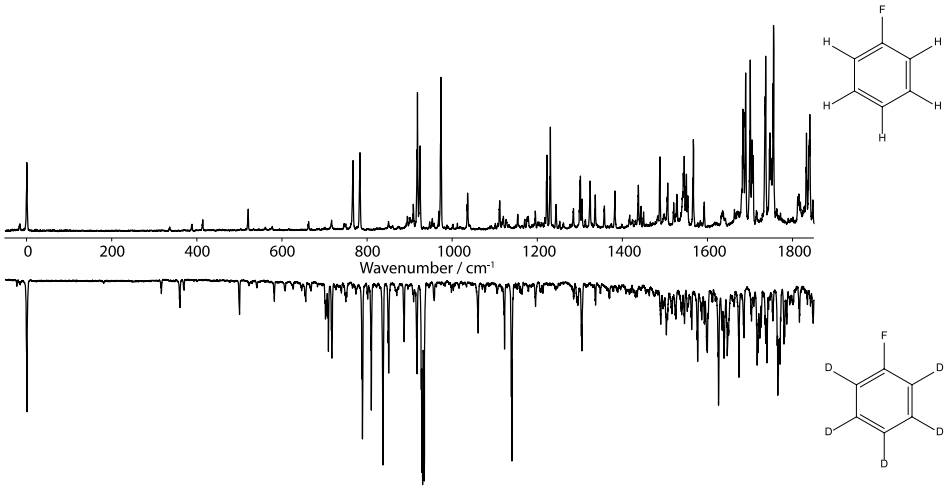

FIG. 1. Complete spectral range scan of the $S_1 \leftarrow S_0$ (1 + 1) REMPI spectrum of FBz-h_5 (top trace, upright) and FBz-d_5 (bottom trace, inverted).

of the rotationless transition in each vibrational feature. For completeness, we note that the maximum in the origin bands occurs at 37 816.8 cm^{-1} and 37 990.8 cm^{-1} for FBz-h_5 and FBz-d_5, respectively. We have not explicitly estimated the rotational temperature in this work, but the observation of the "rotationless dip" indicates a value of around 5 K.

The appearance of the FBz-h_5 spectrum is in good agreement with previously published work;[6,17] however, to the best of our knowledge, there has been no work on FBz-d_5 LIF or REMPI spectra published to date. Lipp and Seliskar did, however, look at the FBz-d_5 isotopologue in absorption,[14] and so we are able to compare to their vibrational band positions. The overall appearance of our FBz-d_5 REMPI spectrum is generally in good agreement with the FBz-h_5 one (see Figure 1), but a number of features shift significantly in wavenumber, as expected—this will be more clearly seen in expanded views, below. The isotopic shifts are clearly mode specific and are dependent upon the extent of participation of the hydrogen atoms in different vibrational modes. Such shifts can lead to changes in the ordering of the vibrations and also in how vibrations can subsequently interact, which depends on their energetic proximity and the efficiency of coupling. A change in ordering would mean that the numbering of the vibrations following the Herzberg (Mulliken) numbering scheme would change. Further below, we shall discuss the assignment of the FBz-h_5 and FBz-d_5 spectra simultaneously, considering different wavenumber regions separately. First, we consider the calculated vibrational wavenumbers and their assignment.

B. Calculated vibrational wavenumbers

The calculated vibrational wavenumbers for FBz-h_5 and FBz-d_5 in the S_0 state are presented in Tables I and II, together with previous experimental values and previous assignments.

1. FBz-h_5 S_0 state

Our calculated B3LYP/aug-cc-pVTZ S_0 vibrational wavenumbers (harmonic values scaled by 0.97) for FBz-h_5 are in very good agreement with the B3LYP/aug-cc-pVDZ ones presented by ourselves in Ref. 4 although the present values should be more accurate. These are also in good agreement with the B3LYP and RICC2 values reported by Pugliesi *et al.*,[6] employing a def2-TZVPP basis set in each case (see Table I). In Ref. 4, we have already discussed the assignment of the S_0 vibrations for FBz-h_5, so it is not discussed here, merely noting that the assignments do not change with the present calculations. In Table I, we also give previous assignments of the FBz-h_5 fundamental vibrations noting the variation in the given Wilson labels; we reiterate that, as pointed out by Pulgliesi *et al.*,[6] Butler *et al.*,[17] and ourselves,[4] Wilson labels are not always a good representation of the motion of the atoms in substituted benzenes. This is re-illustrated in Table I, where the M_i vibrations for FBz-h_5 are expressed as mixed-mode, generalized Duschinsky mixings of the benzene Wilson vibrations. As may be seen, a number of the M_i modes do not even have a dominant contribution from a single Wilson mode.

2. FBz-d_5 S_0 state

We noted in Ref. 4 that when moving from benzene-h_6 to monodeuterated benzene, there was a marked change in the vibrational motions and these became rather mixed, so that some of the C_6H_5D modes were very different from those of C_6H_6. In Figure 2, we show the generalized Duschinsky matrix connecting the S_0 vibrations of FBz-h_5 and FBz-d_5, where it can be clearly seen that there is again significant mixing between the modes.

To gain further insight into this, we investigate how the FBz vibrational wavenumbers change as a function of the artificial mass of the hydrogen atoms as they all simultaneously change from 1 to 2 amu. We do this by calculating the scaled (×0.97) harmonic vibrational wavenumbers for these artificial isotopologues, and producing plots of the wavenumber vs. the mass of the "hydrogen" atom. Such plots are shown in Figure 3 for the S_0 state of FBz, where the vibrations in each C_{2v} symmetry block have been separated for clarity. As noted above, we carried out a similar procedure for benzene in Ref. 4; of

TABLE I. Assignments, mode mixing, and calculated and experimental vibrational wavenumbers (cm^{-1}) for the S_0 state of FBz-h_5.

		Previous assignments			Calculated			Experimental		
Mode label	In terms of benzene modes[a]	Varsányi[b]	Lipp and Seliskar[c]	Butler *et al.*[d]	This work[e]	B3LYP[f]	RICC2[g]	Varsányi[b]	Lipp and Seliskar[c]	Butler *et al.*[d]
					a_1					
M_1	**2**(7a,13)	20a	20a	20a	3107.8	3205.7	3241.7	3100	3094.4	…
M_2	**20a**,7a(13,2)	7a	2	2	3097.2	3194.9	3231.6	3087	3080.2	…
M_3	**13**,7a	2	13	13	3076.7	3174.1	3209.6	3067	3061.0	…
M_4	**9a**	8a	8a	8a	1584.3	1640.1	1631.8	1603	1604.8	…
M_5	**18a**	19a	19a	19a	1481.0	1529.7	1520.2	1499	1500.3	…
M_6	1(12,19a,7a,20a,8a,2,6a,13)	13	7a	7a	1205.6	1248.0	1252.2	1220	1232.4	1239
M_7	**8a**	9a	9a	9a	1140.8	1179.1	1176.6	1156	1156.3	1156
M_8	**19a**(12,1)	18a	18a	18a	1009.7	1042.6	1036.3	1020	1022.7	1023
M_9	**12**,1	12	1	1	992.9	1023.4	1014.3	1009	1008.6	1009
M_{10}	6a(1,12,7a,20a,19a)	1	12	12	799.0	825.1	818.2	806	808.7	810
M_{11}	**6a**(7a,20a)	6a	6a	6a	509.4	526.7	516.5	520	517.1	517
					a_2					
M_{12}	**17a**	17a	17a	17a	954.7	1003.2	962.9	955	957.4	957
M_{13}	**10a**	10a	10a	10a	812.4	874.7	839.1	818	817.6	818
M_{14}	**16a**	16a	16a	16a	413.0	456.7	426.2	[400][h]	413.9	413
					b_1					
M_{15}	**5**,17b	5	5	5	976.5	1014.9	955.1	980	977.8	978
M_{16}	17b,10b(5)	17b	17b	17b	893.2	944.9	901.9	896	894.8	895
M_{17}	11,10b(4)	11	10b	10b	752.3	812.5	770.4	752	754.1	754
M_{18}	**4**,11	4	4	4	677.6	723.6	665.7	685	686.7	687
M_{19}	**16b**,11(10b)	16b	16b	16b	494.6	546.8	512.1	501	497.7	498
M_{20}	**16b**(10b,11,17b,5,4)	10b	11	11	230.4	265.9	238.2	242	248.6	233
					b_2					
M_{21}	**20b**(7b)	20b	…	20b	3105.7	3203.1	3239.4	3053	…	…
M_{22}	**7b**(20b)	7b	7b	7b	3085.2	3183.1	3218.3	3040	3069.5	…
M_{23}	**9b**	8b	…	8b	1593.1	1645.8	1638.8	1597	…	…
M_{24}	**18b**(3)	19b	19b	19b	1445.3	1494.4	1479.5	1460	1460.5	…
M_{25}	15,3	3	3	14	1304.7	1355.7	1429.6	1290	1300.7	…
M_{26}	15,3(8b)	14	…	3	1285.7	1331.8	1321.6	1326	…	1250
M_{27}	**14**,8b	9b	9b	9b	1143.7	1186.6	1177.9	…	1127.7	1128
M_{28}	**19b**(8b,14)	18b	15	15	1058.0	1093.3	1087.6	1066	1066.1	1066
M_{29}	**6b**	6b	6b	6b	608.8	630.9	613.7	615	614.1	614
M_{30}	8b,19b(14,6b,3,18b)	15	18b	18b	394.2	412.5	401.9	405	400.4	404

[a]Note that there have been a number of inconsistencies in applying Wilson labels to some of the modes and often the following switches are required in order for the correct label to be assigned to the correct wavenumber: 8a ↔ 9a, 8b ↔ 9b, 18a ↔ 19a, 18b ↔ 19b, and 3 ↔ 14; however, (as seen in this table) often such labels are a poor representation of the actual mode (see text). Bold entries are dominant contributions: those outside parentheses are ordered major contributions and those inside parentheses are ordered minor contributions—see text.
[b]Reference 7.
[c]References 2 and 15.
[d]Reference 17.
[e]Values scaled by 0.97.
[f]B3LYP/def2-TZVPP from Ref. 6; unscaled.
[g]RICC2/def2-TZVPP from Ref. 6; unscaled.
[h]Estimated value.

pertinence is that significant mixings occurred in the vibrations as the mass of a single hydrogen atom was changed from 1 to 2 amu, i.e., as benzene-h_6 changed into benzene-d_1 (see Figure 3 of Ref. 4).

As may be seen from the present Figure 3, some vibrational modes are more mass-sensitive than others and there is evidence that some of the a_1 and some of the b_2 modes mix and indeed change order in some regions. It may be seen, for example, that there are significant interactions between the M_7, M_8, and M_9 modes. In creating these plots, we assume that vibrations of the same symmetry do not cross, in an analogous way to the non-crossing rule for electronic states of linear molecules; we interpret "avoided crossings" as the occurrence of mixings between vibrations in their vicinity; as the vibrations then move apart again in wavenumber, they revert back to a "pure" mode, albeit at a different vibrational wavenumber and in a different order. Thus, we see that the high → low wavenumber ordering of the a_1 modes has switched from M_7, M_8, and M_9 in FBz-h_5 to vibrations with a major contribution from M_9, M_7, and M_8 in FBz-d_5 (see Table II). In the plot for the b_2 modes in Figure 3, we see that the M_{25} and M_{26} modes are interacting early on, but then separate; thus, we see that in

TABLE II. Assignments, mode mixing, and calculated and experimental vibrational wavenumbers (cm^{-1}) for the S_0 state of FBz-d_5.

Mode label	In terms of FBz-h_5 M_i	Varsányi[a]	Lipp and Seliskar[b]	B3LYP (cm^{-1})[c]	Steele *et al.*[d]	Varsányi[a]	Lipp and Seliskar[b]
			a_1				
$M_1{}^d$	$\boldsymbol{M_1}$	20a	20a	2303.2	2295	2320	…
$M_2{}^d$	$\boldsymbol{M_2}$	7a	2	2290.6	(2275)	…	2291.4
$M_3{}^d$	$\boldsymbol{M_3}$	2	13	2268.6	(2270)	2295	…
$M_4{}^d$	$\boldsymbol{M_4}$	8a	8a	1551.4	1578	1578	1579.2
$M_5{}^d$	$\boldsymbol{M_5}(M_6)$	19a	19a	1371.3	1389	1389	1395.9
$M_6{}^d$	$\boldsymbol{M_6}(M_8, M_5)$	13	7a	1147.8	1163	1163	1172.4
$M_7{}^d$	$\boldsymbol{M_7}(M_8, M_{10}, M_6)$	9a	18a	859.2	880	880	877.2
$M_8{}^d$	$\boldsymbol{M_8}, M_7(M_{10})$	18a	1	807.5	817	817	819.8
$M_9{}^d$	$\boldsymbol{M_9}$	12	9a	951.0	959	959	963.9
$M_{10}{}^d$	$\boldsymbol{M_{10}}(M_8, M_6)$	1	12	740.9	753	753	752.5
$M_{11}{}^d$	$\boldsymbol{M_{11}}$	6a	6a	496.0	505	505	502.8
			a_2				
$M_{12}{}^d$	$\boldsymbol{M_{12}}(M_{14})$	17a	17a	775.8	(789)	(789)	776.2
$M_{13}{}^d$	$\boldsymbol{M_{13}}$	10a	10a	631.9	682	682	636.1
$M_{14}{}^d$	$\boldsymbol{M_{14}}(M_{12})$	16a	16a	359.5	350	350	362.6
			b_1				
$M_{15}{}^d$	$\boldsymbol{M_{15}}(M_{18}, M_{17})$	5	5	815.3	(825)	(825)	…
$M_{16}{}^d$	$\boldsymbol{M_{16}}(M_{15}, M_{17}, M_{19})$	17b	17b	756.4	717	717	759.0
$M_{17}{}^d$	$\boldsymbol{M_{17}}(M_{16}, M_{18}, M_{15})$	4	10b	618.6	627	627	624.7
$M_{18}{}^d$	$\boldsymbol{M_{18}}(M_{17}, M_{15})$	11	4	544.7	563	563	552.9
$M_{19}{}^d$	$\boldsymbol{M_{19}}(M_{17})$	16b	16b	424.2	438	438	426.6
$M_{20}{}^d$	$\boldsymbol{M_{20}}$	10b	11	217.0	229	229	233.7
			b_2				
$M_{21}{}^d$	$\boldsymbol{M_{21}}$	20b	…	2299.4	(2276)	…	…
$M_{22}{}^d$	$\boldsymbol{M_{22}}$	7b	7b	2278.5	(2266)	…	2280.8
$M_{23}{}^d$	$\boldsymbol{M_{23}}$	8b	…	1561.3	1564	1564	…
$M_{24}{}^d$	$\boldsymbol{M_{24}}(M_{28})$	19b	19b	1325.0	1311	1311	1311.7
$M_{25}{}^d$	$\boldsymbol{M_{25}}, M_{26}(M_{24})$	3	3	1020.6	1035	1035	1035
$M_{26}{}^d$	$\boldsymbol{M_{26}}, M_{25}$	14	…	1285.7	1281	1281	…
$M_{27}{}^d$	$\boldsymbol{M_{27}}(M_{28})$	9b	9b	831.3	843	843	843.2
$M_{28}{}^d$	$\boldsymbol{M_{28}}(M_{27}, M_{24})$	18b	15	796.4	806	806	806.7
$M_{29}{}^d$	$\boldsymbol{M_{29}}$	6b	6b	584.2	590	590	591.5
$M_{30}{}^d$	$\boldsymbol{M_{30}}$	15	18b	375.7	388	388	384.9

[a]From Ref. 7.
[b]From Refs. 2 and 15.
[c]Present work; B3LYP/aug-cc-pVTZ values scaled by 0.97.
[d]From Ref. 11 although only generic descriptions of the modes were given. Values in parentheses were estimated by the authors of that work. Note that where a change in ordering of the M_i modes occurs between FBz-h_5 and FBz-d_5, the energetic ordering of the modes has been changed here from that presented in Ref. 11.

FBz-d_5 the ordering of these two modes is the reverse of that in FBz-h_5. All other orderings remain unchanged although there are mixings between the FBz-h_5 modes in forming the FBz-d_5 ones. The latter information forms the Duschinsky matrix in Figure 2, referred to above. The same information has also been summarized in Table II, where the explicit mixings of the FBz-h_5 modes which lead to the FBz-d_5 modes is given, using the notation employed previously,[4] and which is summarized as follows. We call a contribution with a mixing coefficient ≥0.5, a dominant contribution, which is indicated in bold. If the normalized mixing coefficient for a contribution is <0.5 and greater than 0.2, it is listed as a major contribution with no parentheses; if the contribution is between 0.05 and 0.2, then this is counted as a minor contribution and listed inside parentheses. If there is more than one major and/or minor contribution, then these are listed in descending order of importance; contributions <0.05 are ignored. We note that the form of the vibrations calculated in the present work is very close to those of Ref. 4, and so the mixing of the Wilson modes is also the same; the only significant difference we noted was for the M_{25} and M_{26} modes, where the present contributions are somewhat different to those in Ref. 4; the present results are expected to be the more reliable.

For clarity, we designate the vibrational modes of FBz-d_5 as $M_i{}^d$, with the post-superscript d indicating that we are referring to the pentadeuterated molecule, while for overtones and combination bands we add the superscript d outside of parentheses; the lack of such a superscript indicates that we are referring to the FBz-h_5 isotopologue. We note that while Steele *et al.*[11] employed generic descriptions of the FBz-d_5 vibrational modes, Varsányi,[7] and Lipp and Seliskar[2] have employed Wilson-like labels although these are not consistent

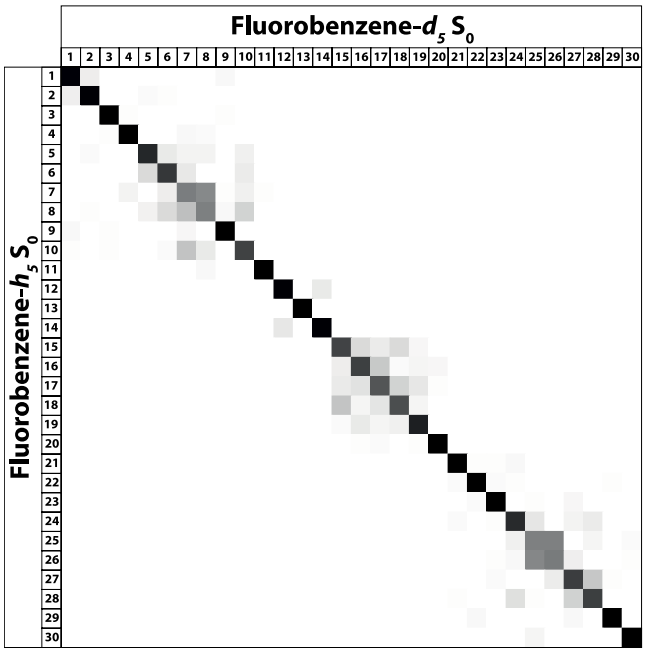

FIG. 2. Generalized Duschinsky matrix showing how the S_0 state FBz-d_5 vibrational modes can be expressed in terms of the FBz-h_5 ones. Black shading indicates a normalized coefficient value of 1.00, while white indicates a value of 0.00, with the level of the grey shading indicating intermediate values. See text.

with each other (see Table II). We also note that the cited values in Varsányi's book are not completely in agreement with those published in Ref. 11, despite this appearing to be the cited source of these. In any case, as can be seen from Table I, Wilson mode labels are not useful in being able to convey the motion of the atoms.

It is clear from Table II that the agreement between the experimental and calculated wavenumber values for the S_0 state of FBz-d_5 is generally good. In a number of cases, the vibrational wavenumber has been estimated by Steele *et al.*,[11] and these values are also in good agreement with the calculated wavenumbers. We also note that Lipp and Seliskar[2] obtained slightly more precise values, not only from vibrational spectroscopy but also from observed hot bands in the electronic transition in the case of a_1 and b_2 symmetry modes,[15] allowing them to deduce the wavenumber of the $M_{29}{}^d$ (ν_{6b}) mode for the first time. The two sets of values agree in the main although we note that the $M_{13}{}^d$ and $M_{16}{}^d$ wavenumbers from Steele *et al.*[11] are in poor agreement with the values from Lipp and Seliskar,[2] with the latter values being in better agreement with our calculated ones. There are other smaller discrepancies between the two sets of data, but we are unable to decide between the cited wavenumbers in these cases.

3. S_1 state

In Tables III and IV we give the calculated TD-DFT B3LYP/aug-cc-pVTZ vibrational wavenumbers for the S_1 states of FBz-h_5 and FBz-d_5. We also give the RICC2/def2-TZVPP calculated values from Ref. 6 for the S_1 state of FBz-h_5 and additionally "isotopically-scaled" versions of these for the S_1 state of FBz-d_5, which we have obtained by applying our calculated TD-DFT B3LYP/aug-cc-pVTZ isotopic shift to the FBz-h_5 S_1 RICC2/def2-TZVPP values of Ref. 6. For FBz-h_5, we find that most of the TD-DFT B3LYP/aug-cc-pVTZ and RICC2/def2-TZVPP vibrational wavenumbers are in good agreement with each other, but several of the low wavenumber modes seem to be more reliably calculated with the latter method, particularly the M_{14} mode; on the other hand, a number of our scaled harmonic values are in better agreement with the experiment than are the RICC2 ones. In the cases where the FBz-h_5 S_1 vibrational wavenumber has been experimentally determined, we also used the ratio between the TD-B3LYP value and the experimental one as a scaling factor to give "experimental scaled" values for FBz-d_5 from its TD-B3LYP values. In assigning the spectra, we looked at all of the different calculated values, but giving weight to the "experimental scaled" values.

In Tables III and IV, we also show how each S_1 vibrational mode may be expressed in terms of the S_0 modes for each of FBz-h_5 and FBz-d_5, using the same syntax as in Tables I and II. This is the usual Duschinsky mixing that can occur between vibrational modes upon electronic excitation. This is represented via shaded Duschinsky matrices in Figure 4.

As noted above, the assignment of the FBz-h_5 $S_1 \leftarrow S_0$ vibrational structure has been discussed by Butler *et al.*,[17] and subsequently by Pugliesi *et al.*,[6] based on LIF and REMPI experiments, respectively, with assignments being confirmed by DF and ZEKE spectroscopy in the respective cases. In the Pugliesi *et al.* paper,[6] some refinements to the assignments of Butler *et al.*[17] were made, particularly emphasising that some modes in the S_1 state were mixtures of the S_0 modes. Indeed, sometimes the mixings were to such an extent that a "composite" notation was employed for some of the S_1 vibrations. We essentially agree with the assignments presented in Refs. 6 and 17 with only minor modifications. For example, we find that the FBz-h_5 S_1 M_{15} and M_{16} modes can be expressed in terms of the S_0 vibrations, with a dominant contribution in each case, and so we label these S_1 modes with the same M_i label as in the ground state; similarly, we find the M_8 and M_9 modes to have corresponding dominant contributions. We agree, however, that the M_{18} and M_{19} modes are each significant mixtures of the corresponding S_0 modes; to highlight this, we label these modes in the S_1 state as $M_{(18/19)a}$ and $M_{(18/19)b}$ in the case of FBz-h_5, with the latter one having the lower wavenumber. We have also noted that the M_{26} mode does not have a dominant contribution, but is highly mixed with the M_{25} mode in S_1, although the M_{25} mode does have a dominant contribution; again we highlight this by representing these as $M_{(25/26)a}$ and $M_{(25/26)b}$. Although there is mode mixing for FBz-d_5, there is always a dominant contribution, and so we assign a unique $M_i{}^d$ label to these, but noting that some of the S_1 modes will be significantly mixed forms of the S_0 ones.

C. Assignment

We now discuss the assignment of the spectrum, breaking the regions down into three wavenumber ranges, and discussing the FBz-h_5 and FBz-d_5 spectra together. In each case, we show expanded views of the spectra, with the FBz-d_5 spectrum inverted for clarity; the spectra are plotted on the same relative wavenumber scale, so that the origins are aligned.

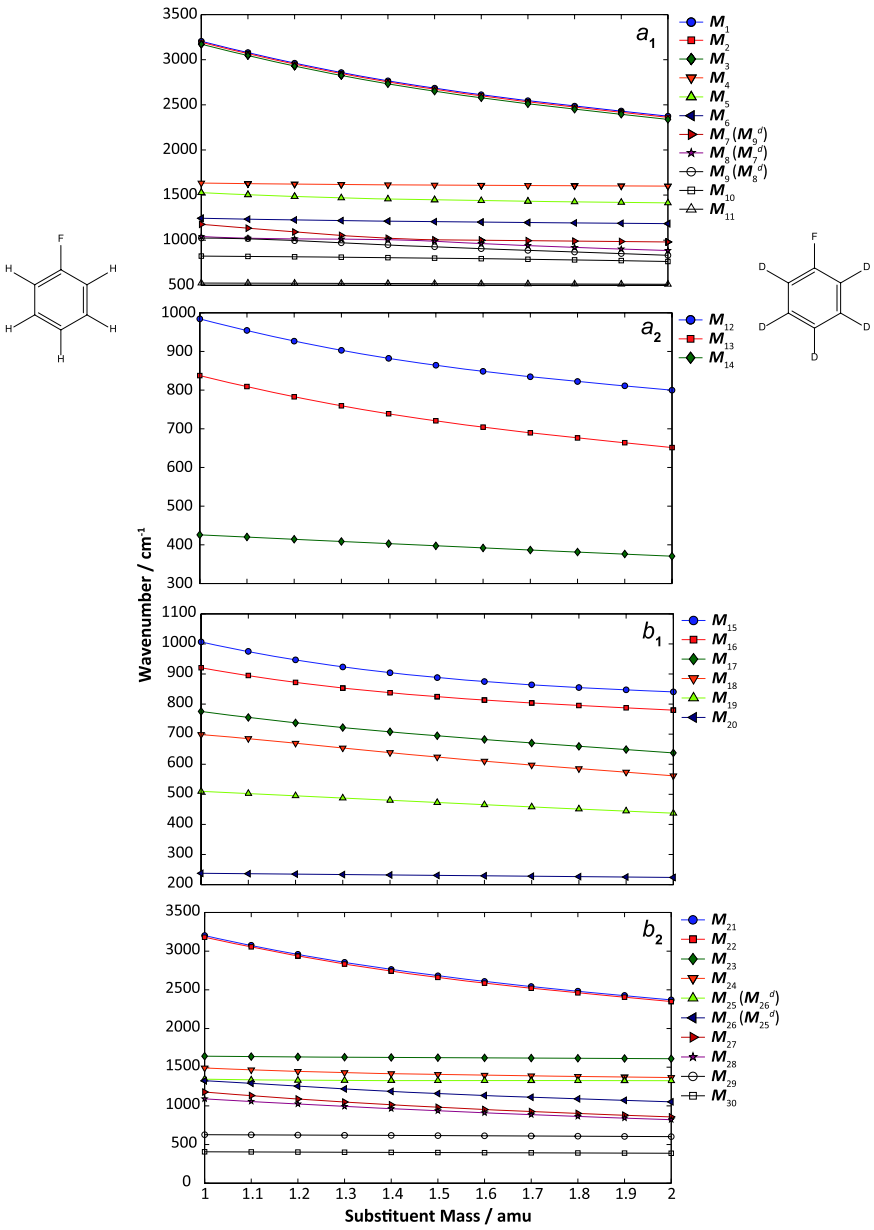

FIG. 3. Plots showing how the S_0 state vibrational wavenumbers of FBz-h_5 (left-hand side) evolve into the values for FBz-d_5 (right-hand side) as a function of the artificial mass of the hydrogen atoms. It has been assumed that vibrations within each symmetry block do not cross. See text. Note that several vibrations change order between the isotopologues, and to highlight this, we have added the M_i^d labels (see text) to the right hand side of the relevant plots.

1. Low wavenumber range (0–550 cm^{-1})

Expanded views of the low-wavenumber ranges of the FBz-h_5 and FBz-d_5 REMPI spectra are presented in Figure 5. In both cases, a strong origin band is observed, with weaker features to higher wavenumber. In agreement with Butler *et al.*[17] and Pugliesi *et al.*,[6] we observe three main bands below 450 cm^{-1} for FBz-h_5, which can be assigned as the M_{20}^2, M_{30}, and M_{14}^2 vibrations, respectively. We agree with Butler *et al.*[17] that the feature at 363.7 cm^{-1} reported by Lipp and Seliskar[14] is not a cold line (in our spectrum we do see weak features around 370 cm^{-1}, but we suspect these are hot bands), and concur that the much stronger line at 335.6 cm^{-1} should be assigned to M_{20}^2. (Lipp and Seliskar[14] did observe the latter band, but did not assign it.) All three of these values are in good agreement with the RICC2 calculated vibrational wavenumbers. We note that our B3LYP value for M_{14} is in poor agreement with the RICC2 one (and with experiment), and suggests that the B3LYP method is unable to describe this motion well; the M_{20} and M_{30} values are, however, in good agreement. We note in passing that our experimental vibrational wavenumber values agree almost exactly with those of Lipp and Seliskar[14] and Butler *et al.*,[17] but we find those of Pugliesi *et al.*[6] are often 3–5 cm^{-1} lower; we are unable to account for these discrepancies.

For FBz-d_5, again three main bands appear in the region < 450 cm^{-1} and these were again observed by Lipp and Seliskar[14] although the lowest wavenumber feature was unassigned by them. Owing to isotopic shifts, the $(M_{14}^2)^d$ vibration now appears in between the $(M_{20}^2)^d$ and M_{30}^d bands. We agree with Lipp and Seliskar[14] in regard to the assignment of the two higher wavenumber features in this region (although they used

TABLE III. Calculated and experimental vibrational wavenumbers (cm^{-1}) for the S_1 state of FBz-h_5.

			Calculated		Experimental			
Mode number	Duschinsky mixing[a]	Mode label	TD-B3LYP[b]	RICC2[c]	Lipp and Seliskar[d]	Butler *et al.*[e]	Pugliesi *et al.*[f]	This work[g]
				a_1				
1	M_1	M_1	3134.3	3262.4	…	…	…	…
2	M_2,M_3	M_2	3118.9	3246.3	…	…	…	…
3	M_3,M_2	M_3	3091.9	3220.6	…	…	…	…
4	M_4	M_4	1513.4	1546.7	…	…	…	…
5	M_5	M_5	1408.9	1431.3	…	…	…	…
6	M_6	M_6	1210.7	1244.0	1220	1230	1220.4	1230.0
7	M_7	M_7	1115.7	1143.5	922	…	…	…
8	M_8,M_9	M_8	932.2	936.1	916	917	911.0	917.8
9	M_9,M_8	M_9	963.2	978.3	968	969	963.0	970.0
10	M_{10}	M_{10}	774.4	780.1	765	765	761.1	766.2
11	M_{11}	M_{11}	459.8	459.4	460	460	457.6	[456.0]
				a_2				
12	M_{12}(M_{13})	M_{12}	622.3	597.1	…	643	…	[643.8]
13	M_{13}(M_{12})	M_{13}	482.5	486.9	…	509	…	[509.2]
14	M_{14}	M_{14}	152.2	208.7	206	206	204.9	[206.6]
				b_1				
15	M_{15}(M_{16},M_{17})	M_{15}	799.5	738.1	…	755	…	[756.0]
16	M_{16}(M_{15})	M_{16}	681.8	610.9	…	661	…	[661.8]
17	M_{17}(M_{15})	M_{17}	588.7	570.9	555	555	…	[555.3]
18	M_{18},M_{19}	$M_{(18/19)a}$	472.4	458.4	…	451	…	[451.7]
19	M_{19},M_{18}	$M_{(18/19)b}$	301.6	333.5	…	331	328.4	[331.1]
20	M_{20}	M_{20}	173.0	174.2	168	168	166.4	[167.8]
				b_2				
21	M_{21}	M_{21}	3130.1	3258.6	…	…	…	…
22	M_{22}	M_{22}	3112.5	3240.0	…	…	…	…
23	M_{23}	M_{23}	1470.5	1691.4	…	…	…	…
24	M_{24}(M_{26})	M_{24}	1382.7	1398.9	…	…	…	…
25	M_{25},M_{26}(M_{24})	$M_{(25/26)a}$	1411.2	1530.9	1589	1589	…	…
26	M_{25},M_{26}	$M_{(25/26)b}$	1265.3	1284.0	…	…	…	…
27	M_{27}	M_{27}	1134.1	1161.7	…	…	…	…
28	M_{28}	M_{28}	982.1	986.9	976	955	…	952.6
29	M_{29}(M_{30})	M_{29}	508.9	514.4	519	518	515.7	520.0
30	M_{30}	M_{30}	381.6	383.7	387	388	385.0	388.0

[a]Duschinsky mixing of the S_0 state vibrations to form the S_1 state ones.
[b]Present work; TD-B3LYP/aug-cc-pVTZ scaled by 0.97.
[c]RICC2/def2-TZVPP values from Ref. 6.
[d]Absorption spectroscopy, Ref. 14.
[e]LIF spectroscopy, Ref. 17.
[f]REMPI spectroscopy, Ref. 6.
[g]Values in square brackets are derived from overtones or combinations bands, other values are from fundamentals. Values in parentheses indicate that the fundamental is part of a Fermi resonance and so the actual position of the fundamental is not definitive. We have given the position of the mid-point of each main feature, on the grounds that these vibrations are expected to be the "bright" states in each case. Their non-perturbed position will, of course, be somewhat different.

Wilson notation). In Table IV, we see that the scaled RICC2 vibrational wavenumber for $M_{14}{}^d$ is consistent with that of the experimental overtone band; both RICC2 and B3LYP methods give good results for the other two features.

An assignment of a very weak band at 457.6 cm^{-1} to M_{11} was made in Ref. 6, with the confirmation coming from both quantum chemical calculations and ZEKE spectroscopy, with the weakness of the feature attributed to little change in geometry along this coordinate in the $S_1 \leftarrow S_0$ transition. However, no such band was seen by Butler *et al.*[17] nor by Lipp and Seliskar.[14] We saw no definitive evidence for this band in the present work nor for any corresponding feature in FBz-d_5.

Towards the end of the respective spectral regions is a strong line for each isotopologue, which is located at 520.0 cm^{-1} for FBz-h_5 and 499.0 cm^{-1} for FBz-d_5; these are assigned as M_{29} and $M_{29}{}^d$, respectively. These correspond to the classic "ν_{6b}" mode of benzene, which appears as a result of vibronic coupling with the second electronically excited state, leading to intensity borrowing and the appearance of the $S_1 \leftarrow S_0$ spectrum of benzene. As is well known, despite the corresponding electronic transition being formally allowed for monosubstituted (and other) benzenes, and so there being no requirement for vibronic coupling, the vibronically induced b_2 symmetry vibrations of benzene are still prevalent in such spectra.

TABLE IV. Calculated and experimental vibrational wavenumbers (cm^{-1}) for the S_1 state of FBz-d_5.

Mode number	Duschinsky mixing[a]	Mode label	TD-B3LYP[b]	RICC2 scaling of TD-B3LYP[c]	Exp. scaling of TD-B3LYP[d]	Lipp and Seliskar[e]	Experiment[f]
				a_1			
1	M_1^d	M_1^d	2320.5	2415.4	…	…	…
2	M_2^d,M_3^d	M_2^d	2301.8	2395.8	…	…	…
3	M_3^d,M_2^d	M_3^d	2279.8	2374.7	…	…	…
4	M_4^d	M_4^d	1475.6	1508.1	…	…	…
5	$M_5^d(M_6^d)$	M_5^d	1291.6	1312.2	…	…	…
6	$M_6^d(M_5^d)$	M_6^d	1134.3	1165.5	1153.6	1137	1139.6
7	M_7^d	M_7^d	832.4	853.1	…	836	…
8	M_8^d	M_8^d	788.8	792.1	774.4	786	788.6
9	M_9^d	M_9^d	919.6	934.0	926.4	932	(931.0)
10	M_{10}^d	M_{10}^d	710.2	715.4	702.0	747	(709.4)
11	M_{11}^d	M_{11}^d	447.9	447.5	444.1	…	…
				a_2			
12	M_{12}^d	M_{12}^d	512.3	491.5	533.8	…	[530.2]
13	M_{13}^d	M_{13}^d	379.7	383.2	406.4	…	[401.6]
14	M_{14}^d	M_{14}^d	129.3	177.3	183.7	179	[179.8]
				b_1			
15	$M_{15}^d(M_{16}^d)$	M_{15}^d	688.9	636.0	645.4	…	[651.3]
16	$M_{16}^d(M_{15}^d)$	M_{16}^d	599.1	536.8	579.1	…	…
17	M_{17}^d	M_{17}^d	466.5	452.4	433.1	…	[443.2]
18	M_{18}^d,M_{19}^d	M_{18}^d	255.3	247.7	234.6	…	[234.2]
19	M_{19}^d,M_{18}^d	M_{19}^d	374.5	414.1	404.0	…	[411.4]
20	M_{20}^d	M_{20}^d	162.3	163.4	157.1	158	[158.1]
				b_2			
21	M_{21}^d	M_{21}^d	2311.5	2406.4	…	…	…
22	M_{22}^d	M_{22}^d	2291.2	2385.0	…	…	…
23	$M_{23}^d(M_{26}^d)$	M_{23}^d	1436.8	1652.6	…	…	…
24	M_{24}^d	M_{24}^d	1222.1	1236.4	…	…	…
25	M_{25}^d	M_{25}^d	1004.1	1018.9	…	…	…
26	$M_{26}^d(M_{23}^d)$	M_{26}^d	1404.4	1523.6	…	…	…
27	$M_{27}^d(M_{28}^d)$	M_{27}^d	818.0	837.9	…	…	…
28	$M_{28}^d(M_{27}^d)$	M_{28}^d	768.5	772.2	739.0	…	739.0
29	M_{29}^d	M_{29}^d	490.7	496.0	501.8	498	499.0
30	M_{30}^d	M_{30}^d	363.7	365.7	370.1	368	369.4

[a]Duschinsky mixing of the S_0 state vibrations to form the S_1 state ones.
[b]Present work; TD-B3LYP/aug-cc-pVTZ values scaled by 0.97.
[c]Used the RICC2-B3LYP ratio in FBz-h_5 to scale the FBz-d_5 B3LYP values.
[d]Used the experimental-TD-B3LYP ratio in FBz-h_5 to scale the FBz-d_5 TD-B3LYP values.
[e]From Refs. 14 and 15.
[f]Values in square brackets are derived from overtones or combinations bands, other values are from fundamentals. Values in parentheses indicate that the fundamental is part of a Fermi resonance and so the actual position of the fundamental is not definitive. We have given the position of the mid-point of each main feature on the grounds that these vibrations are expected to be the "bright" states in each case. Their non-perturbed position will, of course, be somewhat different.

2. Medium wavenumber region (550-1000 cm^{-1})

We now move on to discuss a much "busier" region of the spectrum, particularly for FBz-d_5. The expanded spectra can be seen in Figure 6. We show slightly different medium-wavenumber ranges of the two spectra in Figure 7, where fewer features are marked, but where we emphasise those vibrations that have undergone significant isotopic shifts between the two isotopologues and are discussed below.

a. FBz-h_5. Commencing with FBz-h_5, again the main features have been reported by Lipp and Seliskar,[14] Butler *et al.*,[17] and Pugliesi *et al.*;[6] as such, the assignments of the main features for this isotopologue are well established. We note again that our spacings are in very good agreement with the first two studies, but a number of those from Ref. 6 are a few cm^{-1} too low.

It is straightforward to assign the band at 662.2 cm^{-1}, which was assigned as M_{19}^2 by Butler *et al.*;[17] we agree, however, with Pugliesi *et al.*[6] that the corresponding fundamental vibration is better described as a mixture of the S_0 M_{18} and M_{19} modes, and so we have designated this fundamental as $M_{(18/19)b}$; hence we designate the assignment of this overtone band as $M_{(18/19)b}^2$. The weak band at 715.8 cm^{-1} was assigned as $M_{13}M_{14}$ by Butler *et al.*,[17] which was confirmed by DF, this is confirmed by the RICC2 calculated wavenumbers.

The two very strong lines at 766.2 and 782.8 cm^{-1} are a Fermi resonance between the M_{10} and the combination $M_{(18/19)a}M_{(18/19)b}$, confirmed by the similar structure observed

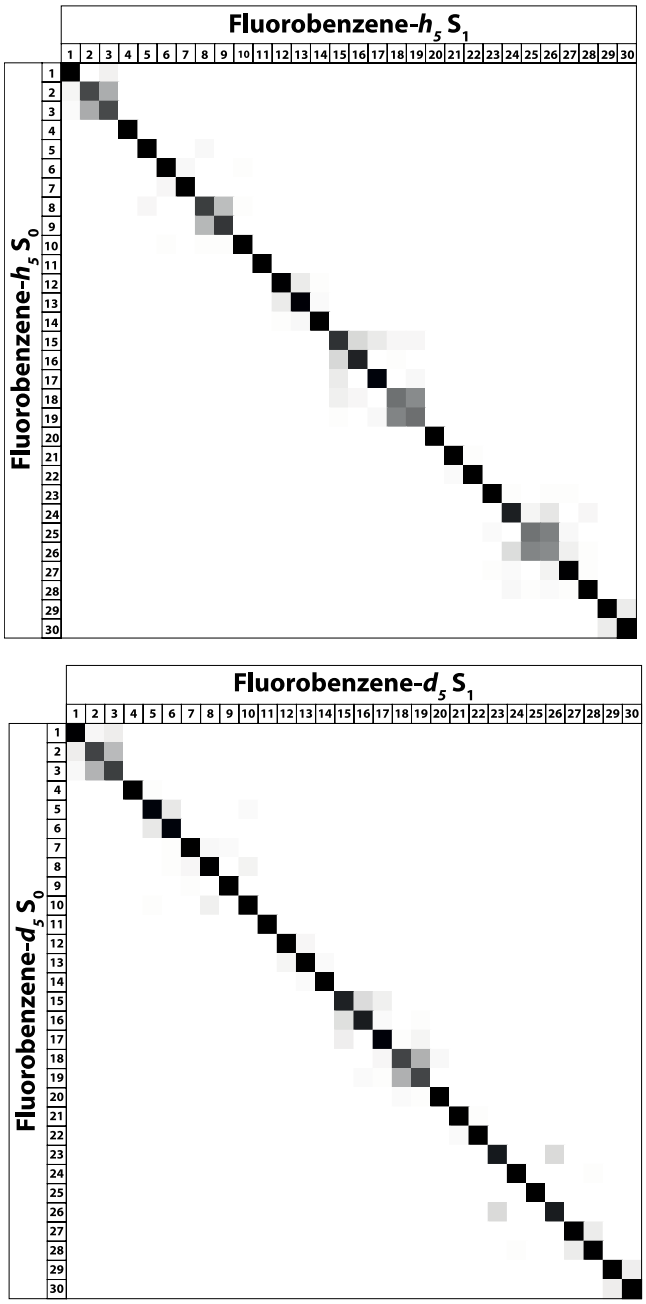

FIG. 4. Duschinsky matrices showing how the S_1 vibrational modes are related to the S_0 ones for FBz-h_5 (top) and FBz-d_5 (bottom). See text. Black shading indicates a normalized coefficient value of 1.00, while white indicates a value of 0.00, with the level of the grey shading indicating the intermediate values. See text.

when dispersing the fluorescence from each feature.[17] This is very similar to the behaviour observed for toluene and toluene-d_3 via dispersed fluorescence[22] and ZEKE spectroscopy,[20] where the same two vibrations are also in Fermi resonance.

b. FBz-d_5. One is immediately struck by the large amount of structure present in the FBz-d_5 spectrum in this region, particularly when compared to that in FBz-h_5. It is therefore surprising to note that in Lipp and Seliskar's paper,[14] they reported no features in the range 500–736 cm^{-1}, while we have many features in this region, including some reasonably intense bands; in particular, we note that none of the features at ~700–720 cm^{-1}, designated Region α in Figure 6, were reported in Ref. 14. In addition, only some of the intense bands were reported in the 770–850 cm^{-1} region.

To assign the FBz-d_5 spectrum, we first note that we expect to see similar vibrational activity in the spectrum of each of the two isotopologues since the change in the equilibrium geometry is the same; however, there will be differences in activity caused by vibrational effects, including vibrations undergoing isotopic shifts, and therefore moving in and out of Fermi resonance with each other. To aid the assignment, we have calculated the vibrational wavenumbers for the S_1 state of FBz-d_5 and present these values in Table IV. Rather than simply relying on the globally scaled (×0.97) TD-B3LYP values, as noted above we also have obtained "RICC2" values for FBz-h_5 from Ref. 6, where we have scaled our FBz-d_5 TD-B3LYP values by the same factor as the ratio of the TD-B3LYP and RICC2 values for FBz-h_5; and additionally, we undertook a similar scaling of the FBz-d_5 TD-B3LYP values using the ratio of the FBz-h_5 TD-B3LYP and the available experimental values. In assigning the FBz-d_5 spectrum, we give most weight to the final set of values, but also use the other two sets of values as a guide, particularly in deducing approximate values for vibrations not observed for the FBz-h_5 isotopologue. All three sets of calculated values are presented in Table IV.

We first consider the $M_{10}/M_{(18/19)a}M_{(18/19)b}$ Fermi resonance seen in FBz-h_5. When we move to FBz-d_5, we can see from the calculated vibrational values in Table IV that the $(M_{18}M_{19})^d$ combination should appear close to 640 cm^{-1}, while the $M_{10}{}^d$ vibration should appear close to 705 cm^{-1}, i.e., these have moved apart significantly owing to the isotopic shifts. We note that there is a weak feature at 645.6 cm^{-1}, which can be assigned to $(M_{18}M_{19})^d$. Its weakness would be in line with the corresponding vibration being optically dark in FBz-h_5 and having gained intensity from M_{10} by Fermi resonance, as suggested by Butler *et al.*;[17] this is also in line with the conclusions reached for toluene,[20,22] where these vibrations are also in Fermi resonance. The calculated wavenumber suggests that $M_{10}{}^d$ is providing the intensity for the features in Region α—see Figures 6 and 7. In Table V we list vibrations that are likely to be contributing to this complicated feature. The expanded view of Region α in Figure 6 indicates that there are three main features, which are likely to consist of contributions from more than one vibration. Since these vibrations are likely to be mixed in a "complex Fermi resonance," we simply offer the probable contributors in Table V. To disentangle this further, and to provide further evidence of the contributing features, dispersed fluorescence or ZEKE spectroscopy could be employed; or, given the energetic proximity of these features, a time-resolved study could be attempted with a picosecond pulse producing a wavepacket consisting of all vibrational eigenstate contributions.[10,23,24]

We note that Lipp and Seliskar[14] assigned a band at 746.8 cm^{-1} to the $M_{10}{}^d$ vibration (ν_{12} in their notation), but as we note, this vibration is calculated to red shift much further than this, and so we do not concur with this assignment. The same authors also assigned a band at 781.4 cm^{-1} for FBz-h_5 as the $M_{30}{}^2$ overtone, but this feature has been shown to be the higher-wavenumber component of the $M_{10}/M_{(18/19)a}M_{(18/19)b}$ Fermi resonance;[17] for FBz-d_5 Lipp and Seliskar[14] attributed a weak band at 736.6 cm^{-1} to the corresponding $(M_{30}{}^2)^d$

TABLE V. Possible assignments for the features in Regions α, β, and γ—see Figure 6.

			Calculated band positions/cm^{-1}				
Region	Feature	Experimental bands (cm^{-1})[a]	B3LYP[b]	RICC2-scaled[c]	Exp.-scaled[d]	Exp.[e]	Possible contributions[f]
	a	701.0	550.2	695.3	708.2	697.5	$(M_{14}{}^3M_{20})^d$ (b_2)
		702.2	710.2	715.4	702.0	…	$M_{10}{}^d$ (a_1)
		703.8	655.3	706.4	710.9	707.3	$(M_{14}M_{20}M_{30})^d$ (a_1)
α		704.8	742.2	737.9	705.9	708.5	$(M_{18}M_{20}{}^3)^d$ (a_1)
	b	708.4	641.6	668.8	717.5	710.0	$(M_{12}M_{14})^d$ (a_1)
	c	716.6	517.2	709.2	734.8	719.2	$(M_{14}{}^4)^d$
		717.8					
			788.8	792.1	774.4	…	$M_8{}^d$
			739.5	788.2	784.9	782.0	$(M_{11}M_{14}M_{20})^d$
			748.3	790.7	788.4	783.4	$(M_{14}M_{18}M_{30})^d$
	d	788.6	835.2	822.2	783.4	784.6	$(M_{18}{}^2M_{20}{}^2)^d$
			851.2	799.4	802.5	…	$(M_{15}M_{20})^d$
	e	800.8	759.4	766.4	812.8	803.2	$(M_{13}{}^2)^d$
			706.5	802.1	811.5	803.7	$(M_{11}M_{14}{}^2)^d$
	f	809.4	802.2	836.1	810.0	806.3	$(M_{14}M_{18}{}^2M_{20})^d$
			754.2	797.3	810.4	813.0	$(M_{13}M_{19})^d$
			854.4	784.5	813.7	813.3	$(M_{16}M_{18})^d$
			811.6	813.2	814.2	813.5	$(M_{11}M_{30})^d$
β			815.3	822.8	816.0	815.2	$(M_{20}{}^2M_{29})^d$
			749.0	828.2	808.0	822.8	$(M_{19}{}^2)^d$
			769.2	850.0	836.6	828.0	$(M_{14}{}^2M_{18}{}^2)^d$
			818.2	813.3	829.1	831.1	$(M_{14}M_{15})^d$
	g	822.2	818.0	837.9	…	…	$M_{27}{}^d$
			832.4	853.1	…	…	$M_7{}^d$
	h	837.0	865.5	858.6	835.8	836.4	$(M_{11}M_{28}M_{20})^d$
			782.3	836.7	842.6	836.9	$(M_{14}M_{20}M_{29})^d$
	i	850.0	874.3	861.1	839.3	837.8	$(M_{18}{}^2M_{30})^d$
			846.2	835.6	839.5	844.8	$(M_{13}M_{17})^d$
			841.0	866.5	837.1	854.6	$(M_{17}M_{19})^d$
			749.3	850.6	869.2	858.6	$(M_{14}{}^2M_{29})^d$
	j		828.4	918.2	901.9	907.4	$(M_{14}M_{19}M_{20}{}^2)^d$
			958.5	942.9	913.3	912.5	$(M_{11}M_{18}{}^2)^d$
		916.6	875.3	921.0	920.1	913.0	$(M_{14}M_{18}M_{29})^d$
			953.4	942.6	904.4	917.5	$(M_{17}M_{20}{}^3)^d$
			800.6	901.2	930.9	919.3	$(M_{13}M_{14}{}^2M_{20})^d$
	k		919.6	934.0	926.4	…	$M_9{}^d$ (a_1)
γ		927.6	795.4	932.1	928.5	929.1	$(M_{14}{}^2M_{19}M_{20})^d$ (a_1)
		928.6	905.7	912.3	933.6	929.1	$(M_{13}M_{20}M_{30})^d$ (a_1)
		929.2	892.0	874.7	940.2	931.8	$(M_{12}M_{13})^d$ (a_1)
		930.6	1021.2	990.8	938.4	936.8	$(M_{18}{}^4)^d$ (a_1)
		933.2	900.5	943.2	931.2	938.9	$(M_{19}M_{20}M_{30})^d$ (b_2)
		934.4	920.4	956.5	931.0	939.2	$(M_{14}M_{17}M_{20}{}^2)^d$ (b_2)
			886.8	905.6	937.8	941.6	$(M_{12}M_{19})^d$ (b_2)

[a]Observed peak positions are given although these will be slightly different to the band origin positions.
[b]TD-B3LYP values scaled by 0.97.
[c]Used the RICC2-B3LYP ratio in FBz-h_5 to scale the FBz-d_5 B3LYP values.
[d]Used the experimental-B3LYP ratio in FBz-h_5 to scale the FBz-d_5 B3LYP values.
[e]These values are based solely on the experimental values when available; otherwise they are a combination of available experimental values and exp.-scaled values for vibrations that were not observed. The possible assignments are ordered by this column.
[f]Overall symmetries are given for the possible contributions to the more-complicated features.

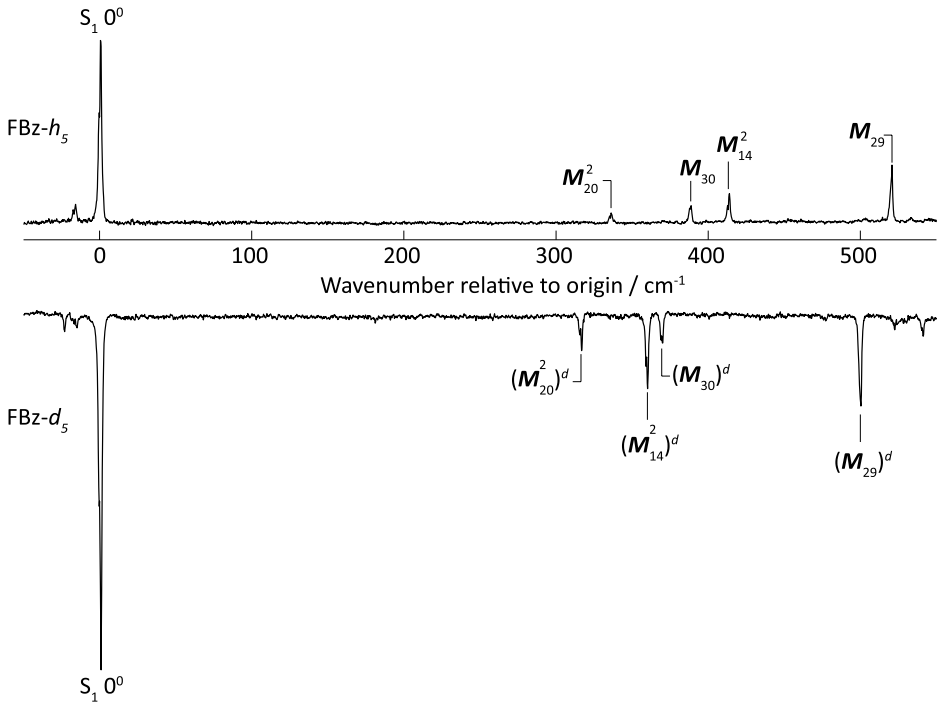

FIG. 5. Expanded views of the low wavenumber regions (0–550 cm^{-1}) of the $S_1 \leftarrow S_0$ (1 + 1) REMPI spectra of FBz-h_5 (top trace, upright) and FBz-d_5 (bottom trace, inverted).

transition, but we see no definitive evidence of a feature at this wavenumber, and have assigned a different feature to this vibration.

Moving up higher in wavenumber, we note that there are four intense bands (d, f, h, and i) in the wavenumber range 780–860 cm^{-1}, designated Region β in Figure 6, with two additional, much weaker associated features. Although it is difficult to be sure which of these bands were observed by Lipp and Seliskar,[14] bands d and h seem to be among these, while somewhat surprisingly, the strong bands f and i were not.

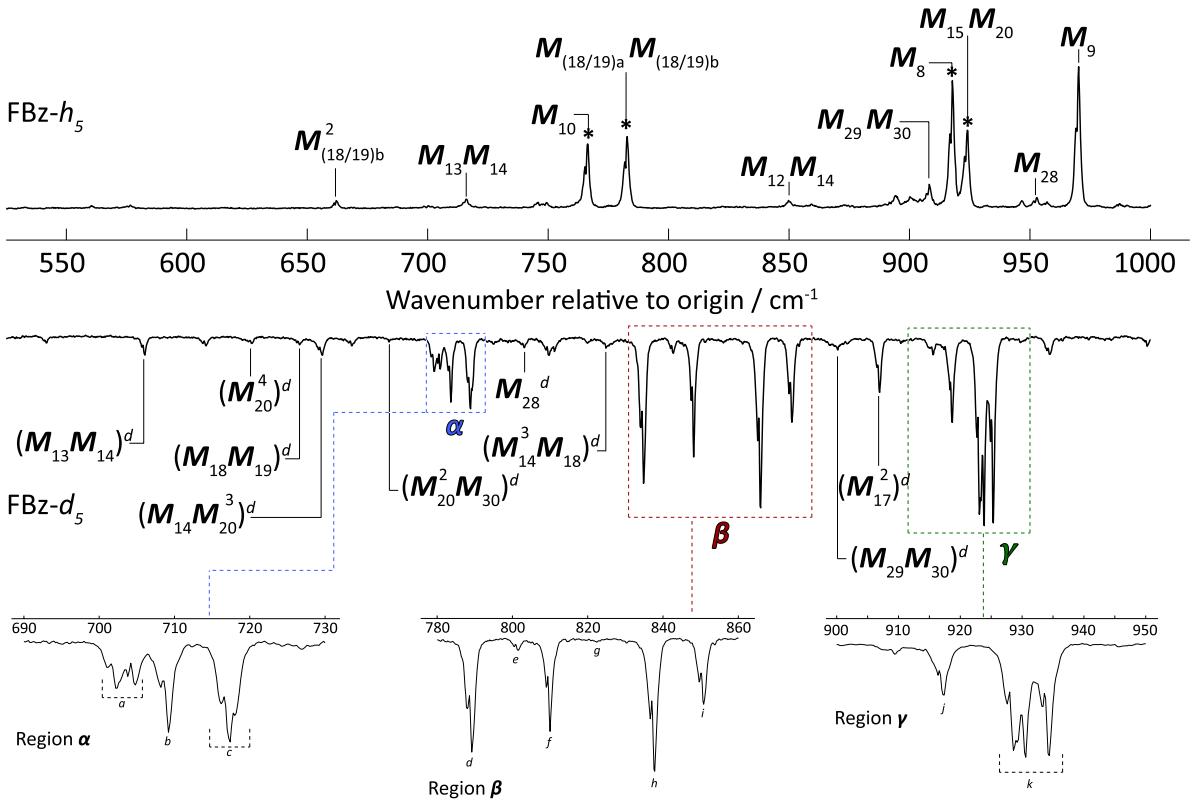

FIG. 6. Expanded views of the medium wavenumber regions (550–1000 cm^{-1}) of the $S_1 \leftarrow S_0$ (1 + 1) REMPI spectra of FBz-h_5 (top trace, upright) and FBz-d_5 (bottom trace, inverted). The zoomed-in sections at the bottom are those for Regions α, β, and γ of FBz-d_5, which are indicated by coloured dashed boxes in the main spectrum. See text for further details.

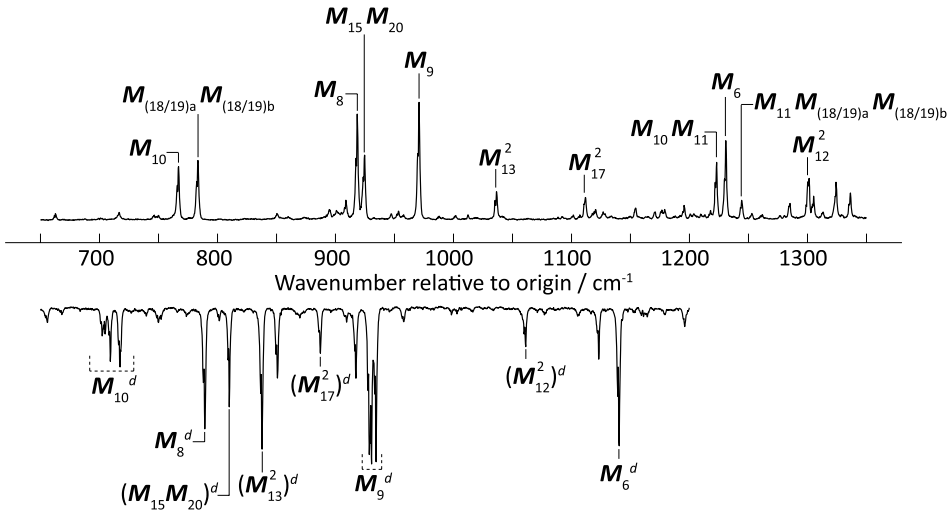

FIG. 7. Slightly extended scans of the spectral regions in Figure 6, emphasising those vibrations that undergo significant isotopic shifts between the two isotopologues. Our favoured assignments of three of the most intense bands in Region β (see Figure 6) are given, with the fourth such band not having a definitive assignment (see text). For Regions α and γ (see Figure 6), we simply indicate each of the vibrations that we hypothesise is providing the bulk of the intensity to these regions (see text).

To investigate the assignment possibilities, we calculated vibrational wavenumbers for fundamentals, combinations, and overtones in this region (values presented in Table IV) which have a_1 or b_2 symmetry; we present the resulting values in Table V. We particularly note that bands *d*, *f*, *h*, and *i* are quite intense, and so we would expect that there would likely be corresponding relatively intense bands also in the FBz-h_5 isotopologue spectrum. There are no obvious candidates very close in wavenumber, and so we looked for strong features in the FBz-h_5 spectrum that could isotopically shift into this range—see Figure 7. With this in mind, it seems clear that we should expect the $M_8{}^d$ vibration, which we expect to lie in the 775–790 cm^{-1} range from the calculated values, which would fit the position of band *d* very well, and even though there are other possibilities for this feature, there is no other strong feature that would fit the $M_8{}^d$ vibration so well. We also note that the $(M_{15}M_{20})^d$ vibration is expected in this wavenumber region, and so it seems likely that one of bands, e or f, is due to this combination, and we shall return to this shortly.

Further perusal of the FBz-h_5 spectrum, and the list of bands that should appear in this spectral region, indicates that we should certainly expect to see the $(M_{13}{}^2)^d$ and the $(M_{17}{}^2)^d$ vibrations—see Figure 7. Since we expect the $(M_{17}{}^2)^d$ vibration to appear at 865–900 cm^{-1}, we favour the assignment of the band at 886.4 cm^{-1} to this overtone. The $(M_{13}{}^2)^d$ vibration should appear somewhere in the range 765–815 cm^{-1}, and is expected to be one of the more intense bands. Although the agreement is not as close as could be desired, the only reasonable choice is to assign band *h* to $(M_{13}{}^2)^d$, with the discrepancy attributable to deficiencies in the calculated scaled values, and perhaps also shifts due to Fermi resonance. The two less intense bands, *f* and *i*, may then be assigned as vibrations that gain intensity from Fermi resonance with $M_8{}^d$ and $(M_{13}{}^2)^d$ states being the optically bright ones, respectively. In Table V, we show possibilities for these vibrations, but it is difficult to be definitive without further evidence. Currently, we favour band *f* as being assignable to $(M_{15}M_{20})^d$ on the grounds that band *e* is so weak (and given the intensity of $M_{15}M_{20}$ in the spectrum of FBz-h_5). We acknowledge that the separation of $M_8{}^d$ and $(M_{15}M_{20})^d$ is now more than for the corresponding features in FBz-h_5, which might lead to a diminution of the intensity of the latter; this could be less of an issue if the $(M_{15}M_{20})^d$ vibration had some inherent bright character, but this has not been definitively established. The weakness of the M_{11} feature (not actually observed in the present work) in FBz-h_5 and FBz-d_5 would be in line with band *e* being assigned to $M_{11}M_{14}{}^2$ (gaining some intensity from Fermi resonance), but other assignments are also possible (see Table V). If we take the assignment of band *h* as $(M_{13}{}^2)^d$ and assume that band *i* arises from Fermi resonance, then that would exclude the assignment of this feature to $(M_{14}{}^2M_{29})^d$, for example, as it does not have a_1 symmetry; assignments to $M_7{}^d$ or $(M_{17}M_{19})^d$ would be possible, with a gain in intensity from the Fermi resonance in FBz-d_5 perhaps being the explanation for their non-observance in the FBz-h_5 spectrum.

The next section of the spectrum contains a complicated feature consisting of a number of overlapping features, with a more isolated band to lower energy at 916.6 cm^{-1}; we designate this section as Region γ (see Figure 6). The complicated feature, labelled *k*, corresponds well to the expected position of the $M_9{}^d$ vibration, which is intense in the case of FBz-h_5—see Figure 7, with there being no other obvious intense band expected in this region. We thus conclude that there are several bands in a complex Fermi resonance in the 927–935 cm^{-1} wavenumber range, with candidates listed in Table V. Clearly, if $M_9{}^d$ is the main intensity carrier, then we only expect bands of a_1 symmetry to gain intensity from Fermi resonance, but there are still several of these. Again, further evidence from ZEKE spectroscopy, dispersed fluorescence or time-resolved studies will be required to unravel the complicated interactions. Likely candidates for the weaker feature at 916.6 cm^{-1} are also listed in Table V.

3. High energy region

Above Region γ, there are reasonably intense features that can be relatively straightforwardly assigned to $(M_{12}^2)^d$ at 1060.4 cm^{-1} and $M_6{}^d$ at 1139.6 cm^{-1}, both of which red shift from their positions in FBz-h_5 (see Figure 7). In addition, there is a band at 1122.2 cm^{-1}. We considered the assignment of this band to the $(M_{10}M_{11})^d$ combination band based on the fact that it is also expected to red shift, and it is known to interact with the M_6 mode in FBz-h_5. We note, however, that this assignment is unlikely, since the derived value for M_{11} would then be too far from the calculated value to be comfortable. A better assignment would appear to be to $(M_{15}M_{20}{}^3)^d$ whose expected wavenumber is very close to that observed. If this assignment is correct, it suggests that the $(M_{10}M_{11})^d$ vibration has now moved too far away from $M_6{}^d$ to interact appreciably, and so now is very weak. On the other hand, the $M_{15}M_{20}{}^3$ combination does not obviously appear in the FBz-h_5 spectrum, and so its appearance in FBz-d_5 suggests that it is in Fermi resonance with M_6 and so gaining intensity from it.

Another interesting difference is also present for FBz-d_5: the $(M_{11}M_{18}M_{19})^d$ combination band does not appear although a corresponding feature is relatively intense in FBz-h_5 (Figure 7). [Note that in Table 1 of Ref. 17 the $M_{11}M_{18}M_{19}$ band is incorrectly entered as $M_{10}M_{18}M_{19}$ although it is clear that this is an error from the other cited values; this has been confirmed with the principal author of that paper.] In fact, the explanation for the appearance of the $M_{11}M_{18}M_{19}$ combination band in FBz-h_5 was that M_{10} and $M_{18}M_{19}$ are in Fermi resonance, and therefore their combinations with the M_{11} ought also to be in Fermi resonance (although the couplings will not be identical). As noted above, the $(M_{18}M_{19})^d$ vibration has shifted appreciably upon isotopic substitution, and therefore is no longer in Fermi resonance with $M_{10}{}^d$; as a consequence, the $(M_{11}M_{18}M_{19})^d$ band is also not seen in this spectral region.

Lipp and Seliskar[14] report a value for $M_6{}^d$ (designated ν_{7a} in their work) at 1137.3 cm^{-1}, which is in very good agreement with the value of 1139.6 cm^{-1} from the present work; however, we note that the intensity of this band relative to the origin is reported as being rather low, while in the present work the $M_6{}^d$ feature is somewhat more intense than the origin, and this can only partially be attributed to dye intensity variation. Again, there is a missing feature, with 1122.2 cm^{-1} feature not having been reported by them. As with the other "missing" features from Lipp and Seliskar's paper (see above), we have no explanation for the differences regarding these two spectral features.

Clearly, there are many features in the high energy region for both isotopologues, with the 1500–1800 cm^{-1} region being particularly dense for FBz-d_5 (see Figure 1). For FBz-h_5, a number of these have been assigned by Butler *et al.*[17] and they particularly noted the consistency of extrapolating the lower wavenumber assignments to higher energy with overtones and combination bands—even including those of the Fermi resonances. Of course, the higher in energy one goes, the more likely, and the more complex, these Fermi resonances will become. In the high wavenumber region of the FBz-d_5 spectrum (see Figure 1, inverted trace), it can be seen that the high energy region has become very dense, and assigning this region will be very involved. In addition, it could be argued that this becomes more and more of a fruitless task as the vibrations become mixtures of ever-increasing numbers of fundamentals, so that gaining insight into the specific motions of the atoms is ever-less informative.

TABLE VI. A summary of the assigned features from the present work for the $S_1 \leftarrow S_0$ transition in FBz-d_5.

Experimental bands (cm^{-1})[a]	Assignment[b]
316.2	$(M_{20}{}^2)^d$
359.6	$(M_{14}{}^2)^d$
369.4	$M_{30}{}^d$
499.0	$M_{29}{}^d$
581.4	$(M_{13}M_{14})^d$
626.0	$(M_{20}{}^4)^d$
645.6	$(M_{18}M_{19})^d$
654.6	$(M_{14}M_{20}{}^3)^d$
667.4	...
683.6	$(M_{20}{}^2M_{30})^d$
701.0 *a*	$[(M_{14}{}^3M_{20})^d]$
702.2 *a*	$[M_{10}{}^d]$
703.8 *a*	$[(M_{14}M_{20}M_{30})^d]$
704.8 *a*	$[(M_{18}M_{20}{}^3)^d]$
708.4 *b*	$[(M_{12}M_{14})^d]$
716.6 *c*	$[(M_{14}{}^4)^d]$
717.8 *c*	...
726.8	$(M_{14}{}^2M_{30})^d$
739.0	$M_{28}{}^d$
749.8	...
773.6	$(M_{14}{}^3M_{18})^d$
788.6 *d*	$[M_8{}^d]$
800.8 *e*	*
809.4 *f*	$[(M_{15}M_{20})^d]$
822.2 *g*	$[M_{27}{}^d]$
837.0 *h*	$[(M_{13}{}^2)^d]$
850.0 *i*	$[M_7{}^d]$
866.4	...
869.6	$(M_{29}M_{30})^d$
886.4	$(M_{17}{}^2)^d$
916.6 *j*	$(M_{17}M_{20}{}^3)^d$
927.6 *k*	*
928.6 *k*	*
929.2 *k*	*
930.6 *k*	$[M_9{}^d]$
933.2 *k*	*
934.4 *k*	*
957.0	$[(M_{18}M_{19}M_{20}{}^2)^d]$
1006.4	$[(M_{18}M_{19}M_{14}{}^2)^d]$
1015.6	$[(M_{18}M_{19}M_{30})^d]$
1060.4	$(M_{12}{}^2)^d$
1122.2	$(M_{15}M_{20}{}^3)^d$
1139.6	$M_6{}^d$

[a]The letters correspond to the peaks identified in Figure 6 and in Table V, and which are discussed in the text.

[b]Assignments in square brackets are those which are less certain, due to a number of possibilities for the feature, but which are thought to be the most sensible of the selection available. Asterisks indicate bands where there are many possible assignments. These are given for certain features in region γ, and the possible assignments for these features are given in Table V.

V. SUMMARY AND CONCLUSIONS

In this work, we have presented the $S_1 \leftarrow S_0$ electronic spectra of both FBz-h_5 and FBz-d_5 up to ~1800 cm^{-1}. There are very interesting aspects to these spectra, which are highlighted by the fact that there is only a simple mass change between the two isotopologues; however, the impact on the spectra is marked.

We first note that there is an issue with comparing vibrations between the two isotopologues. Not only does the vibrational wavenumber change markedly for some of the vibrations, but also the form of the vibration changes significantly. This is demonstrated by the motions of the S_0 FBz-d_5 vibrations not having a 1:1 correspondence with the FBz-h_5 ones, but rather some of these become quite mixed forms of significantly more than one vibration, with several not being identifiable with any single FBz-h_5 mode. This is reminiscent of the changes in vibration in going from benzene to (mono)fluorobenzene, as pointed out by Butler *et al.*,[17] and perhaps more explicitly by Pugliesi *et al.*[6] In Ref. 4, we highlighted that heavy perturbation of some vibrational modes actually occurs on going from benzene to monodeuterated benzene; hence, it is not surprising that such mixing occurs for the present isotopologues. Despite this, the main changes in vibration that occur for each isotopologue upon electronic excitation from the S_0 state to the S_1 state are rather similar—this is the classic Duschinsky mixing.

Assigning the FBz-d_5 spectrum is straightforward, for the most part, since we expect largely the same vibrational activity as in FBz-h_5; however, as we have shown, there are significant differences caused by vibrations (fundamentals, combinations, and overtones) coming in and out of resonance as a result of the isotopic shifts. This leads to different Fermi resonances being seen although some of those noted in FBz-h_5 persist in FBz-d_5. There are several cases where we are unable to be unambiguous in the assignment, owing to the rapid build-up of the number of vibrations with wavenumber. In these cases, firmer assignment will have to await ZEKE, dispersed fluorescence, or time-resolved studies for confirmation. In Table VI we provide a summary of the assignments made in the present work.

We are unable to explain the absence of mention, in the work of Lipp and Seliskar,[14] of a number of the intense features we observe for FBz-d_5. Both REMPI and absorption spectroscopy should be similarly affected by any photophysical process that could be affecting relative linestrengths (in contrast, say, to LIF) and so this makes the discrepancy between the present work and Ref. 14 all the more surprising. It is unfortunate that the actual spectrum was not reproduced in Ref. 14 for comparison.

In future work, as we have previously undertaken for *para*-fluorotoluene[25] and toluene,[10,20] we hope to undertake ZEKE spectroscopic studies to confirm some of the less secure assignments. We also intend to perform standard and two-dimensional dispersed fluorescence experiments and the results of these will be complementary to the ZEKE ones.

ACKNOWLEDGMENTS

We are grateful to the EPSRC for funding (Grant Nos. EP/I012303/1 and L021366/1) and for a studentship to J.P.H. The EPSRC and the University of Nottingham are thanked for studentships to A.A. and W.D.T. We are grateful to the NSCCS for the provision of computer time under the auspices of the EPSRC, and to the High Performance Computer resource at the University of Nottingham.

[1]D. H. Whiffen, J. Chem. Soc. **1956**, 1350.
[2]E. D. Lipp and C. J. Seliskar, J. Mol. Spectrosc. **73**, 290 (1978).
[3]M. Scotoni, S. Oss, L. Lubich, S. Furlani, and D. Bassi, J. Chem. Phys. **103**, 897 (1995).
[4]A. M. Gardner and T. G. Wright, J. Chem. Phys. **135**, 114305 (2011).
[5]E. B. Wilson, Jr., Phys. Rev. **45**, 706 (1934).
[6]I. Pugliesi, N. M. Tonge, and M. C. R. Cockett, J. Chem. Phys. **129**, 104303 (2008).
[7]G. Varsányi, *Assignments of the Vibrational Spectra of Seven Hundred Benzene Derivatives* (Wiley, New York, 1974).
[8]G. Herzberg, *Molecular Spectra and Molecular Structure II: Infrared and Raman Spectra of Polyatomic Molecules* (Krieger, Malabar, 1991), p. 272.
[9]R. S. Mulliken, J. Chem. Phys. **23**, 1997 (1955).
[10]A. M. Gardner, A. M. Green, V. M. Tame-Reyes, V. H. K. Wilton, and T. G. Wright, J. Chem. Phys. **138**, 134303 (2013).
[11]D. Steele, E. R. Lippincott, and J. Xavier, J. Chem. Phys. **33**, 1242 (1960).
[12]S. H. Wollman, J. Chem. Phys. **14**, 123 (1946).
[13]R. Vasudev and J. C. D. Brand, J. Mol. Spectrosc. **75**, 288 (1979).
[14]E. D. Lipp and C. J. Seliskar, J. Mol. Spectrosc. **87**, 242 (1981).
[15]E. D. Lipp and C. J. Seliskar, J. Mol. Spectrosc. **87**, 255 (1981).
[16]A. Boatwright, N. A. Besley, S. Curtis, R. R. Wright, and A. J. Stace, J. Chem. Phys. **123**, 021102 (2005).
[17]P. Butler, D. B. Moss, H. Yin, T. W. Schmidt, and S. H. Kable, J. Chem. Phys. **127**, 094303 (2007).
[18]J. R. Gascooke, U. N. Alexander, and W. D. Lawrance, J. Chem. Phys. **134**, 184301 (2011).
[19]M. J. Frisch, G. W. Trucks, H. B. Schlegel, G. E. Scuseria, M. A. Robb, J. R. Cheeseman, G. Scalmani, V. Barone, B. Mennucci, G. A. Petersson, H. Nakatsuji, M. Caricato, X. Li, H. P. Hratchian, A. F. Izmaylov, J. Bloino, G. Zheng, J. L. Sonnenberg, M. Hada, M. Ehara, K. Toyota, R. Fukuda, J. Hasegawa, M. Ishida, T. Nakajima, Y. Honda, O. Kitao, H. Nakai, T. Vreven, J. A. Montgomery, Jr., J. E. Peralta, F. Ogliaro, M. Bearpark, J. J. Heyd, E. Brothers, K. N. Kudin, V. N. Staroverov, R. Kobayashi, J. Normand, K. Raghavachari, A. Rendell, J. C. Burant, S. S. Iyengar, J. Tomasi, M. Cossi, N. Rega, J. M. Millam, M. Klene, J. E. Knox, J. B. Cross, V. Bakken, C. Adamo, J. Jaramillo, R. Gomperts, R. E. Stratmann, O. Yazyev, A. J. Austin, R. Cammi, C. Pomelli, J. W. Ochterski, R. L. Martin, K. Morokuma, V. G. Zakrzewski, G. A. Voth, P. Salvador, J. J. Dannenberg, S. Dapprich, A. D. Daniels, Ö. Farkas, J. B. Foresman, J. V. Ortiz, J. Cioslowski, and D. J. Fox, Gaussian 09, Revision C.01 (Gaussian, Inc., Wallingford, CT, 2009).
[20]A. M. Gardner, A. M. Green, V. M. Tame-Reyes, K. L. Reid, J. A. Davies, V. H. K. Parkes, and T. G. Wright, J. Chem. Phys. **140**, 114038 (2014).
[21]I. Pugliesi and K. Muller-Dethlefs, J. Phys. Chem. A **110**, 4657 (2006), a free download of the software can be found at http://www.fclab2.net.
[22]C. G. Hickman, J. R. Gascooke, and W. D. Lawrance, J. Chem. Phys. **104**, 4887 (1996).
[23]J. A. Davies, A. M. Green, A. M. Gardner, C. D. Withers, T. G. Wright, and K. L. Reid, Phys. Chem. Chem. Phys. **16**, 430–443 (2014).
[24]J. A. Davies, A. M. Green, and K. L. Reid, Phys. Chem. Chem. Phys. **12**, 9872 (2010).
[25]V. L. Ayles, C. J. Hammond, D. E. Bergeron, O. J. Richards, and T. G. Wright, J. Chem. Phys. **126**, 244304 (2007).